

Underpotential Deposition of Al-Ce Alloys at an Al Electrode from LiCl-KCl-CeCl₃ Melts

Zhang Meng^{1,2}, Li Yunna², Han Wei², Zhang Milin², Xue Yun^{1,2}, Wang Yanli²,
Gao Yang¹

¹Fundamental Science on Nuclear Safety and Simulation Technology Laboratory, Harbin Engineering University, Harbin 150001, China; ²Key Laboratory of Superlight Materials and Surface Technology, Ministry of Education, Harbin Engineering University, Harbin 150001, China

Abstract: Electrochemical behavior of Ce(III) and underpotential deposition of Al-Ce alloys were investigated at an Al active electrode in LiCl-KCl-CeCl₃ melts. Compared with the cyclic voltammetry curves on a Mo electrode, the redox potential of Ce(III)/Ce at the Al electrode is more positive; there are two new plateaus between the deposition plateau of Al and Ce metal by open circuit chronopotentiometry, which means two kinds of intermetallic compounds. All above show Ce(III) forms intermetallic compound by underpotential deposition electrochemically. Furthermore, it is also confirmed by Al-Ce alloys, which are obtained at the Al active electrode in LiCl-KCl-CeCl₃ melts after potentiostatic deposition under the same condition. The formation of AlCe and AlCe₃ is illuminated by X-ray diffraction (XRD). The reasons of AlCe and AlCe₃ formation were explained by XRD and phase diagram of Al-Ce. The standard Gibbs free energies of AlCe and AlCe₃ formation were calculated by XRD and open circuit chronopotentiometry. The analysis of scanning electron microscopy (SEM) and energy dispersive spectrometry (EDS) reveals that cerium exists at the surface of Al electrode to form an Al-Ce alloys layer, which is about 28 μm in thickness, and evenly coated the Al electrode.

Key words: LiCl-KCl melts; underpotential deposition; Al electrode; Al-Ce alloy

Compared with a traditional method of separation actinides (An) by hydrometallurgical process from fission products (FPs), pyrochemical reprocessing has been considered as a promising alternative due to its compactness, criticality control benefits, resistance to radiation effects, compatibility with advanced fuel types, and the ability to produce low purity products to prevent nuclear proliferation^[1-3]. Because An and lanthanides (Ln) have similar chemical properties, it is an essential and challenging issue to efficient separation of An over Ln in FPs^[4-8].

Since the operation conditions influence the efficiency of

reprocess and the structure of the separation cell, it is important to know the electrochemical behaviors of An and Ln on different electrodes for the understanding of the process^[9]. We use aluminum to recover An group metals according to the thermodynamic calculations to separate An from Ln efficiently^[10-12]. The An have already been separated selectively by electrolysis on solid Al active cathodes in the LiCl-KCl melts, and formed An-Al alloys at the same time^[13].

In previous experiments, R. Malmbeck and co-workers have succeed in electrodeposition of U-Al alloys^[14], Pu-Al alloys^[15], U-Pu-Al alloys^[16], and An-Al alloys^[10] on solid

Received date: August 14, 2015

Foundation item: High Technology Research and Development Program of China (2011AA03A409); National Natural Science Foundation of China (51104050, 91326113, 21271054, 21173060); Natural Science Foundation of Heilongjiang Province of China (E201413); China Postdoctoral Science Foundation (20110491029); Heilongjiang Postdoctoral Fund (LBH-Z10208); Heilongjiang Educational Commission Foundation (12513045); the Fundamental Research Funds for the Central Universities (HEUCF161501); the Scientific Technology Bureau of Harbin (2012RFQXS102); the Basic Research Foundation of Harbin Engineering University (HEUFT08031)

Corresponding author: Han Wei, Ph. D., Professor, Key Laboratory of Superlight Materials and Surface Technology, Ministry of Education, Harbin Engineering University, Harbin 150001, P. R. China, E-mail: happymeng1980@126.com

Copyright © 2016, Northwest Institute for Nonferrous Metal Research. Published by Elsevier BV. All rights reserved.

Al cathodes in the LiCl-KCl melts. While, Y. Castrillejo and co-workers have succeed in extracting Pr, Dy, Gd, Er, Ho, Eu, Lu, Tm, Yb and Sm on the Al electrodes from molten chlorides in the form of Al-Ln alloys^[17].

Cerium is not only a typical element of the FPs, but also a surrogate for studying the behavior of uranium in molten salts^[18,19]. Therefore, it is essential to study the electrochemical property of Ce(III) in LiCl-KCl melts. On an inert electrode, several prior investigations have been conducted on the thermodynamic properties, kinetic reaction parameters and electrochemical behavior of CeCl₃ in molten LiCl-KCl melts, such as the structure^[20], diffusion coefficient^[21-23], the standard potential^[19, 24-26] and rate constant^[19, 27, 28]. Compared with these data on an inert electrode, there are only a few reports on an Al cathode. Y. Castrillejo *et al.* reported the electrodeposition of Al-Ce alloys on Al cathode without XRD pattern analysis^[29]. Furthermore, Ce can form intermetallic compound such as Al-Ce alloy with Al according to Al-Ce phase diagram^[30, 31].

On the basis of these backgrounds, we propose to investigate the electrochemical behavior of Ce(III) by cyclic voltammetry and open circuit chronopotentiometry, and the formation of Al-Ce alloys on Al cathode in LiCl-KCl melts. The results will help us to further study the cerium extraction from molten salts via electroreduction.

1 Experiment

The LiCl (99.0%) and KCl (99.5%) mixture with composition LiCl:KCl=58.8:41.2 (mol%) were melted in an alumina crucible (Volume=150 cm³) and then dried by an electric tubular heater. The temperature of the mixture was measured with a nickel-chromium thermocouple which had an alumina scabbard. Water and metal ion impurities were removed by drying and pre-electrolysis. Anhydrous CeCl₃ (≥99.0%) powder was introduced into the bath in order to provide cerium ions. All experiments were carried out under a nitrogen atmosphere.

All electrochemical measurements were implemented by an Im6eX electrochemical workstation (Zahner Co., Ltd.) with a THALES 3.08 software package. The reference electrode was manufactured by immersing a silver wire ($d=0.5$ mm) into a quartz tube which contained a solution of AgCl (1 wt%) in LiCl-KCl (58.8:41.2, mol%) melts. The working electrode was Mo wire ($d = 1$ mm, 99.99% purity) or Al (99.99% purity), which was polished thoroughly using SiC paper, and then placed in ethanol to clean by ultrasound. A spectrally pure graphite rod ($d = 6$ mm) was used as the counter electrode which was polished as the method mentioned before use. The active electrode surface was determined by measuring the immersion depth of the electrode in the melts at each time.

2 Results and Discussion

2.1 Cyclic voltammetry

Cyclic voltammogram (CV) of LiCl-KCl-CeCl₃ melts at the Mo (curve 1, dotted line) and Al (curve 2, solid line) electrode is shown in Fig.1. The different electrochemical signals obtained at Al and Mo electrode are obvious. At the Al electrode, there are three cathodic peaks marked as A₂, B₂ and C₂. The peaks C₂'/C₂ correspond to the Al oxidation/reduction, which have been pointed out by Wei^[32]. The reduction potential value of Li⁺ (peak B₂) is more positive at the Al electrode than that at the Mo electrode (peak B₁), which has also been observed by Castrillejo^[29].

The electrodeposition peak of Ce(III) on Al and Mo electrode is A₂ and A₁, respectively. The onset potential value of A₂ is -1.25V, which is more positive than the potential of A₁ (-1.78V). It is likely to be caused by the underpotential deposition (UPD) of cerium on aluminum substrate. During this process, AlCe_x alloys are formed according to Al-Ce phase diagram^[30], as the following reaction (1):



During the reverse scan, an anodic peak A₂' which corresponds to Ce dissolution from the AlCe_x is observed.

2.2 Open circuit chronopotentiometry

An EMF measurement was as follows: first, electrodeposition of Ce metal at the Al electrode by constant potential electrolysis was at -2.20 V (vs. Ag/AgCl) for 10 s. After that, a transient curve where the open-circuit potential was recorded versus time on Al electrode at 843K is shown in Fig.2. At the beginning, the potential stays at around -2.08 V (plateau 1), which is generated by pre-deposited Li metal on the electrode. Then, 4 potential plateaus (plateaus 2-5) are observed at -1.91, -1.29, -1.14 and -0.95 V, respectively. Among them, the plateaus 2 and 5 are interpreted as the pre-deposited Ce and Al metals, respectively. Since the deposited Ce metal reacts with Al

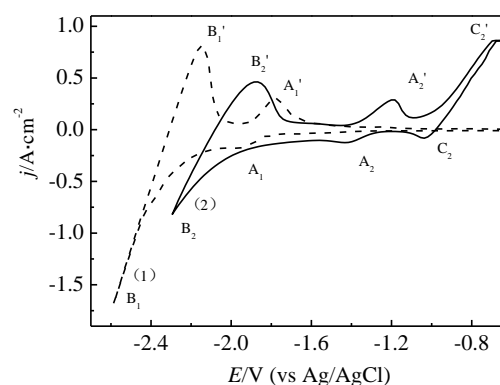


Fig.1 Curves of the LiCl-KCl melts containing 0.96×10^{-4} mol cm⁻³ CeCl₃ on a molybdenum electrode ($S = 0.944$ cm²) (dotted curve) and on an Al electrode ($S = 2.3$ cm²) (solid curve) at 843 K with a scan rate of 0.1 V s^{-1}

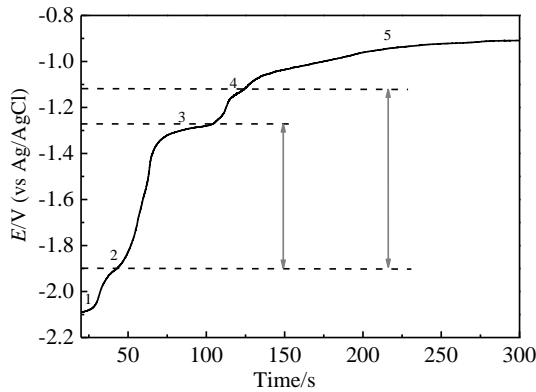


Fig.2 Open circuit transient curve for the Al electrode after electrodepositing at -2.20 V vs. Ag/AgCl for 10 s at 843 K

and diffuses into Al electrode, the electrode potential gradually shifts to more positive values. During this process, a potential plateau should be observed when the composition of the electrode surface is within a range of two-phase coexisting state^[31-36]. Therefore, the plateaus 3 and 4 (at about -1.29 and -1.14 V, respectively) correspond to the mixture of two different AlCe_x alloys.

2.3 Underpotential deposition of Al-Ce alloys at an Al electrode

Based on the results of CV and open-circuit potential, potentiostatic electrolysis was carried out in LiCl-KCl-CeCl₃ melts on an Al electrode at 843 K for 1 h at -1.60 V versus Ag/AgCl. Fig.3 shows the XRD pattern of this sample. At this potential, except for Al (PDF#65-2869), two other peaks are observed as AlCe₃ (PDF#65-1825) and AlCe (PDF#29-0011). At this electrolytic potential, Ce cannot be electrodeposited but Al-Ce alloys can form on the electrode. Once again it confirms that Ce(III) can be reduced by UPD.

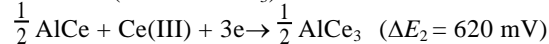
According to the phase diagram^[30] of Al-Ce, except for AlCe₃ and AlCe, the formation temperatures of other Al-Ce alloys are higher than the experimental temperature. Therefore, only two kinds of AlCe₃ and AlCe alloys are obtained under this experimental condition.

The results of XRD patterns accord with open circuit transient curve. The potential plateaus could be considered to correspond to the following two-phase composition and reactions:

Plateau 4 (Al + AlCe):



Plateau 3 (AlCe + AlCe₃):



The formation reactions of AlCe and AlCe₃ are described as the following reactions (2) and (3). Therefore, the standard Gibbs free energies of AlCe and AlCe₃ alloys at 843 K can be calculated.

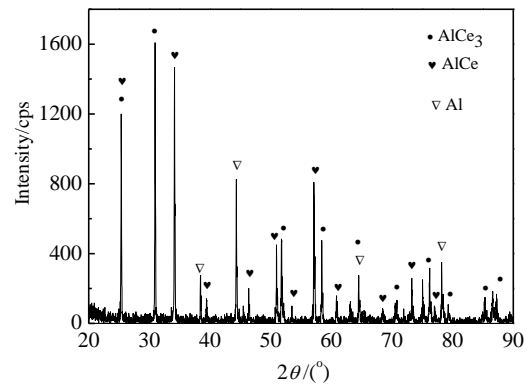
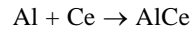
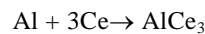


Fig.3 XRD patterns of deposits obtained under potentiostatic electrolysis (-1.60V vs. Ag/AgCl) at 843 K for 1 h



$$\Delta G_{\text{f(AlCe)}}^{\circ} = -3F\Delta E_1 \quad (2)$$



$$\Delta G_{\text{f(AlCe}_3)}^{\circ} = 2\left(\frac{1}{2}\Delta G_{\text{f(AlCe)}}^{\circ} - 3F\Delta E_2\right) \quad (3)$$

where, *F* is faraday constant, then the $\Delta G_{\text{f(AlCe)}}^{\circ}$ and $\Delta G_{\text{f(AlCe}_3)}^{\circ}$ are -222.88 kJ mol⁻¹ and -581.89 kJ mol⁻¹ by open circuit chronopotentiometry, respectively.

According to the data^[37] of standard heat and standard entropy at 298 K, the calculated standard Gibbs energies of reactions (2) and (3) at 843 K are calculated to be -155.08 and -287.18 kJ mol⁻¹, respectively, which are smaller than the experimental values. However, based on our knowledge, standard Gibbs free energies of AlCe and AlCe₃ alloys have not been calculated by experimental method so far.

The cross-sections of Al-Ce alloys after potentiostatic electrolysis at 843 K for 1 h are presented in Fig.4. A layer of about 28 μm in thickness is evenly coated on Al electrode. EDS mapping analysis of element Ce and Al are show in Fig.5b and 5c. From the mapping analysis of elements, we can observe that the element cerium mainly disperses homogenously along the surface of the electrode.

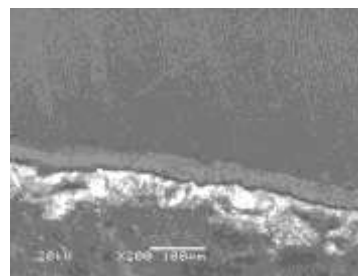


Fig.4 SEM image for Al-Ce alloy by potentiostatic electrolysis (-1.6 V vs. Ag/AgCl) at 843 K for 1 h

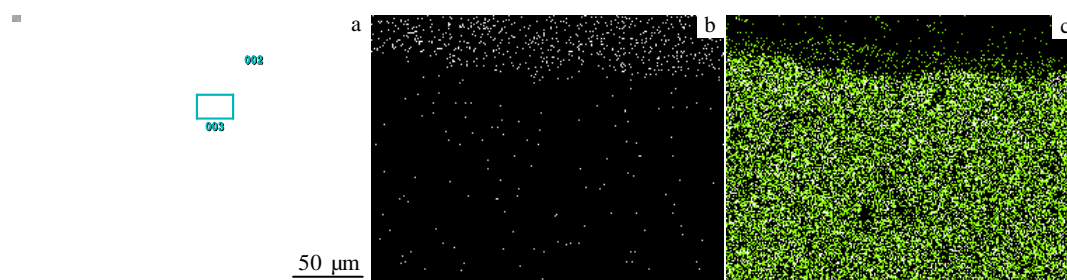


Fig.5 SEM image (a) and EDS mapping analyses of element Ce (b) and element Al (c) for Al-Ce alloy by potentiostatic electrolysis (-1.6 V vs. Ag/AgCl) at 843 K for 1 h

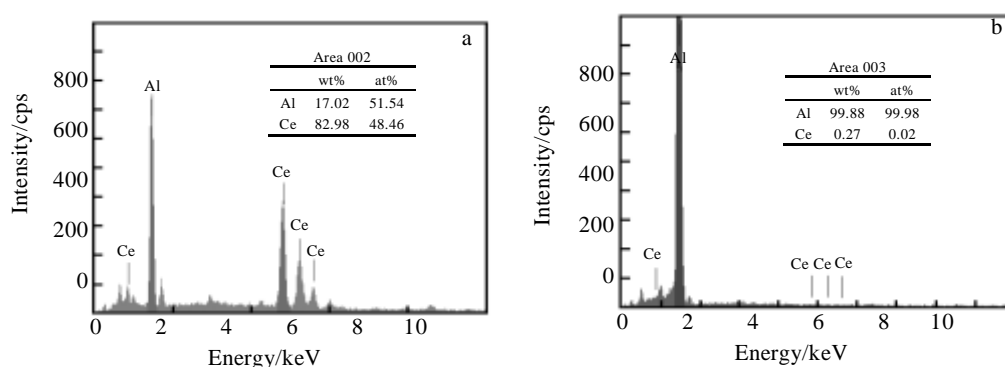


Fig.6 EDS spectra of area 002 (a) and area 003 (b) corresponding to Fig.5a for Al-Ce alloy by potentiostatic electrolysis (-1.6 V vs. Ag/AgCl) at 843 K for 1 h

Fig.6 shows EDS results corresponding to Fig.5a. The areas labeled as 002 and 003 taken from the white zone (the layer) and black zone (the resin), respectively, indicate that the deposit is composed of cerium and aluminum elements. Therefore, the sample prepared by potentiostatic electrolysis is AlCe_x alloys. According to the EDS results, the layer dissolves more Ce (82.98 wt% at area 002) than the resin does (0.27 wt% at area 003). Based on the binary phase diagram of Al-Ce system, Ce, as a surface active element, reacts with Al to form different intermetallic compounds^[10]. During the solidification process, Al-Ce compounds mainly distribute at the surface of the Al electrode.

3 Conclusions

1) The underpotential deposition of Al-Ce Alloys at an Al electrode from LiCl-KCl-CeCl_3 melts can be elucidated by electrochemical methods. The redox potential of the Ce(III)/Ce on Al active electrode has more positive potential values than those on an Mo electrode. The phenomenon is thermodynamically explained by lowering of cerium activity in the metal phase due to the formation of intermetallic compounds.

2) The Al-Ce alloys are prepared in LiCl-KCl-CeCl_3

melts at 843 K by constant potential electrolysis on an Al electrode. XRD illuminates that AlCe and AlCe_3 are formed. The reasons of formation AlCe and AlCe_3 alloys can be explained by XRD and phase diagram of Al-Ce. The standard Gibbs free energies of formation AlCe and AlCe_3 alloys can be calculated by open circuit chronopotentiometry.

3) The cerium exists at the surface of Al electrode to form a thickness uniform Al-Ce alloy layer, and the layer of about 28 μm in thickness is evenly coated on Al electrode.

References

- 1 Liu Kui, Liu Yalan, Yuan Liyong *et al.* *Electrochimica Acta*[J], 2013, 109: 732
- 2 Bermejo M R, de la Rosa F, Barrado E *et al.* *Journal of Electroanalytical Chemistry*[J], 2007, 603: 81
- 3 Taxil P, Massot L, Nourry C *et al.* *Journal of Fluorine Chemistry*[J], 2009, 130: 94
- 4 Liu Yalan, Yuan Liyong, Liu Kui *et al.* *Electrochimica Acta*[J], 2014, 120: 369
- 5 Toda T, Maruyama T, Moritani K *et al.* *Journal of Nuclear Science and Technology*[J], 2009, 46: 18
- 6 Moriyama H, Seshimo T, Moritani K *et al.* *Journal of Alloys and Compounds*[J], 1994, 213: 354

- 7 Moriyama H, Yamana H, Nishikawa S et al. *Journal of Nuclear Materials*[J], 1997, 247: 197
- 8 Mukaiyama T, Takano H, Ogawa T et al. *Progress in Nuclear Energy*[J], 2002, 40: 403
- 9 Castrillejo Y, Bermejo M R, Pardo R et al. *Journal of Electroanalytical Chemistry*[J], 2002, 522(2): 124
- 10 Cassayre L, Malmbeck R, Masset P et al. *Journal of Nuclear Materials*[J], 2007, 360: 49
- 11 Lebedev V A. *Selectivity of Liquid Metal Electrodes in Moltenhalides* (Title translated)[M]. Russian: 1993: 229
- 12 Conocar O, Douyere N, Glatz J P et al. *Nuclear Science and Engineering*[J], 2006, 153: 253
- 13 Serp J, Allibert M, Le Terrier A et al. *Journal of the Electrochemical Society*[J], 2005, 152: 167
- 14 Cassayre L, Soucek P, Mendes E et al. *Journal of Nuclear Materials*[J], 2011, 414(1): 12
- 15 Mendes E, Malmbeck R, Nourry C et al. *Journal of Nuclear Materials*[J], 2012, 420: 424
- 16 Soucek P, Cassayre L, Eloiardi R et al. *Journal of Nuclear Materials*[J], 2014, 447: 38
- 17 Yang Yusheng, Zhang Milin, Han Wei et al. *Electrochimica Acta*[J], 2014, 118: 150
- 18 Yan Yongde, Xu Yanlu, Zhang Milin et al. *Journal of Nuclear Materials*[J], 2013, 433: 152
- 19 Marsden K C, Pesic B. *Journal of the Electrochemical Society*[J], 2011, 158(6): 111
- 20 Betancourt R, Nattland D. *Chemical Physics*[J], 2005, 7(1): 173
- 21 Castrillejo Y, Bermejo M, Millan R et al. *Progress in Molten Salt Chemistry I*[M]. New York: Elsevier, 2000, 143
- 22 Iizuka M. *Journal of the Electrochemical Society*[J], 1998, 145: 84
- 23 Wang Changshui, Liu Yi, He Hui et al. *Journal of Rare Earths*[J], 2013, 31(4): 405
- 24 Fusselman S P, Roy J, Grimmett D et al. *Journal of the Electrochemical Society*[J], 1999, 146(7): 2573
- 25 Lantelme F, Cartailier T, Berghoute Y et al. *Journal of the Electrochemical Society*[J], 2001, 148(9): 604
- 26 Zhang Meng, Han Wei, Zhang Milin et al. *Journal Rare Earths*[J], 2013, 31(6): 609
- 27 Kim T, Ahn D H, Paek et al. *International Journal of the Electrochemical Science*[J], 2013, 8: 9180
- 28 Zhang Meng, Han Wei, Zhang Milin et al. *Chemical Research in Chinese Universities*[J], 2014, 30(3): 489
- 29 Castrillejo Y, Bermejo R, Mart'nez A M et al. *Journal of Nuclear Materials*[J], 2007, 360: 32
- 30 Buschow K H J, Van Vucht J H N. *Philips Res Rep*[J], 1967, 22: 233
- 31 Iizukaa M, Inouea T, Shiraib O et al. *Journal of Nuclear Materials*[J], 2001, 297: 143
- 32 Wei Shuquan, Zhang Milin, Han Wei et al. *Electrochim Acta*[J], 2011, 56: 4159
- 33 Konishi H, Nishikiori T, Nohira T et al. *Electrochimica Acta*[J], 2003, 48: 1403
- 34 Nohira T, Kambara H, Amezawa K et al. *Journal of the Electrochemical Society* [J], 2005, 152: 183
- 35 Bermejo M R, Barrado E, Mart'nez A M et al. *Journal of Electroanalytical Chemistry*[J], 2008, 617(1): 85
- 36 Yan Yongde, Tang Hao, Zhang Milin et al. *Electrochimica Acta*[J], 2012, 59: 531
- 37 Kang Y B, Pelton A D, Patrice C et al. *Computer Coupling of Phase Diagrams and Thermochemistry*[J], 2008, 32: 413

在 LiCl-KCl-CeCl₃ 熔盐中铝电极上欠电位沉积制备 Al-Ce 合金

张 萌^{1,2}, 李云娜², 韩 伟², 张密林², 薛 云^{1,2}, 王艳力², 高 杨¹

(1. 哈尔滨工程大学 核安全与仿真技术国防重点学科实验室, 黑龙江 哈尔滨 150001)

(2. 哈尔滨工程大学 超轻材料与表面技术教育部重点实验室, 黑龙江 哈尔滨 150001)

摘 要: 在 843 K LiCl-KCl-CeCl₃ 熔盐中活性铝电极上, 研究了 Ce(III)离子的电化学反应行为和欠电位沉积 Al-Ce 合金。对比循环伏安曲线发现, 在 Al 电极上 Ce(III)/Ce 反应的氧化还原电势比在 Mo 惰性电极上更正; 开路计时电位在金属铝和铈的沉积平台之间出现 2 个平台, 这表明 Ce(III)在 Al 活性电极上可以生成两种金属间化合物。以上结果在电化学机理上说明 Ce(III)离子可以在 Al 电极上欠电位沉积形成金属间化合物。在该实验条件下通过恒电位电解, 在 Al 电极上得到了 Al-Ce 合金, 验证了电化学分析的结果。经 XRD 表征, 证实形成了 AlCe 和 AlCe₃ 两种合金, 结合 Al-Ce 合金相图分析了只产生这两种合金的原因; 结合开路电位计算了生成这两种合金的标准吉布斯自由能变值。经 SEM 和 EDS 表征, 证明了铈在 Al 电极表面分布, 并形成厚度均一约 28 μm 的 Al-Ce 合金镀层。

关键词: LiCl-KCl 熔盐; 欠电位沉积; 铝电极; Al-Ce 合金

作者简介: 张 萌, 女, 1980 年生, 博士, 副教授, 哈尔滨工程大学核科学与技术学院, 黑龙江 哈尔滨 150001, 电话: 0451-82519702, E-mail: happymeng1980@126.com